

DOI:10.4067/S0718-221X2022005XXXXXX

1
2
3 **PRELIMINARY EVALUATION OF THE INCORPORATION OF**
4 **CELLULOSE NANOFIBERS AS REINFORCEMENT IN WATERBORNE**
5 **WOOD COATINGS**

6 **Tawani Lorena Naide** ^{1a*}, **Pedro Henrique Gonzalez de Cademartori** ^{2b}, **Silvana Nisgoski**
7 ^{2c}, **Graciela Inés Bolzon de Muñiz** ^{2d}

8 ¹ Federal University of Parana, Post-Graduate Program of Forest Engineering, Parana, Brazil.

9 ² Federal University of Parana, Department of Forest Engineering and Technology, Parana,
10 Brazil.

11 ^a <https://orcid.org/0000-0001-6171-0629>

12 ^b <https://orcid.org/0000-0003-3295-6907>

13 ^c <https://orcid.org/0000-0001-9595-9131>

14 ^d <https://orcid.org/0000-0003-4417-0178>

15 ***Corresponding author:** tawnaide@gmail.com

16 **Received:** May 11, 2021

17 **Pre-Accepted:** August 22, 2022

18 **Posted online:** August 23, 2022

19 **ABSTRACT**

20 The wood is exposed to possible damages caused by weather, requiring the application of a
21 finishing coat to provide extra protection. The aim of this work was to evaluate the influence
22 of the addition of microfibrillated cellulose in waterborne varnish on the colorimetric
23 parameters, wettability and finish characteristics of wood products. Color was evaluated with a
24 CM-5 spectrophotometer; surface wettability was analyzed by contact angle measurement
25 using a drop shape analysis goniometer; and abrasion, adhesion and impact tests were
26 performed to evaluate the quality of the coating. The coating's optical characteristics were not
27 affected by the addition of microfibrillated cellulose. The changes in wood wettability were
28 small, with no statistical difference between the wood treated with plain varnish and that with
29 unbleached microfibrillated cellulose. In the analysis of the variation of the contact angle during
30 the elapsed time, the coating containing unbleached microfibrillated cellulose presented the best
31 results. The results of finish quality did not show numerical changes after the addition of the
32 microfibrillated cellulose, but qualitatively the microfibrillated cellulose caused better
33 anchoring of the coating to the specimens. Therefore, the use of microfibrillated cellulose as
34 reinforcement in coatings has potential, but tests with different consistencies and tests of other
35 properties are necessary.

36 **Keywords:** Colorimetry, microfibrillated cellulose, waterborne coating, wettability, wood
37 finish.

38 INTRODUCTION

39 Wood is a porous and hygroscopic material, so its appearance and structural integrity
40 can vary according to moisture content due to absorption and desorption of water, resulting in
41 reduced durability and/or increased development of fungi, among other characteristics (Gezici-
42 Koç *et al.* 2018, Kluge *et al.* 2017). That is why it is necessary to use coating materials, such as
43 varnish, to extend the service life of wood as well as to enhance decorative aspects.

44 According to the use of the wood, it could be defined whether it will be necessary to
45 apply a preservative product or whether a surface coating is sufficient. If the wood is intended
46 for more rigorous applications in an aggressive environment, it is necessary to use preservative
47 products that must be efficient against the intended disadvantages and must be discarded at the
48 end of their useful life without presenting any environmental risk (Yona *et al.* 2021). For
49 purposes where the wood is not in a hostile environment, it is recommended to apply an
50 appropriate coating, which when interacting and adhering to the wood substrate, will form a
51 coating film that can extend the service life of the products, reducing the impact of degraders
52 agents, providing changes in the visual aspect and preserving its original performance (Žigon
53 2021, Gibbons *et al.* 2020).

54 While in the past, processing, performance and price characteristics were the main
55 determining factors for the development of coating materials, in recent decades, environmental
56 and health aspects have been considered increasingly important (Veigel *et al.* 2014). More
57 stringent regulations regarding the use of volatile organic compounds (VOCs) have caused
58 solvent-based coatings to be progressively replaced by waterborne coatings (Duan *et al.* 2016,
59 Tan *et al.* 2016). However, because the latter are more sensitive to water, depending on the
60 intended use of the final product it is necessary to increase the coatings' mechanical properties,
61 which can be done by inclusion of fillers and other additives.

62 Due to their morphology, nanofibers have a very large surface-to-volume ratio, which
63 allows them to interact strongly with the environment and improve the mechanical properties
64 of polymeric matrices. Furthermore, their nanometric scale mostly preserves the transparency
65 of the coating. In particular, cellulose nanofibers, i.e. microfibrillated cellulose (MFC) has a
66 polar and reactive surface, in addition to having substantially lower hardness, strength and
67 rigidity than inorganic nanoparticles, making it promising to replace inorganic fillers and
68 additives (Kluge *et al.* 2017, Veigel *et al.* 2014).

69 The good potential of cellulose nanofibers is based on the possibility of its use as
70 reinforcement in composite materials, but this depends on adequate dispersion in the matrix
71 (Islam *et al.* 2013). Since cellulose is hydrophilic in terms of surface chemistry, it disperses
72 well in aqueous media, generating a homogeneous mixture (Kluge *et al.* 2017). Nanocellulose
73 combines important properties of cellulose, such as hydrophilicity, chemical modification
74 capacity and formation of fibers with semicrystalline morphology.

75 The present study investigated the possibility of adding MFC, as filler in waterborne
76 wood coatings, by evaluating the influence on colorimetric characteristics, wood wettability
77 and on the properties of resistance to impact, adhesion and abrasion of the coating applied to
78 the wood.

79 **MATERIALS AND METHODS**

80 **Preparation and characterization of microfibrillated cellulose**

81 Industrial kraft pulp from *Pinus* spp. (bleached and unbleached) was used. Moisture
82 content was determined by gravimetry to calculate the percentage of pulp and water necessary
83 to prepare nanocellulose with a consistency of 2 % by dry weight. Microfibrillated cellulose
84 was obtained by mechanical processing in a defibrillator mill (Masuko Sangyo
85 Supermasscolloider MKCA6-3) using 10 passes and a constant frequency of 157,08 rad/s
86 (Potulski *et al.* 2016, Silva *et al.* 2019).

87 MFC morphology was evaluated by transmission electron microscopy (TEM) with a
88 JEOL JEM 1200EX-II microscope, with resolution of 0,5 nm, magnification range of up to 600
89 kX and voltage of up to 120 kV, equipped with a Gatan high-resolution CCD camera (Orius
90 SC1000B).

91 The crystallinity index of cellulose and MFC was determined with an X-ray
92 diffractometer (Shimadzu XRD-7000) applying the method of Segal *et al.* (1959). This method
93 involves applying equation 1 to calculate the crystallinity index based on the ratio between the
94 intensity of the crystalline peak and the intensity of amorphous regions.

$$95 \quad ICr = \frac{I_{002} - I_{am}}{I_{002}} * 100 \quad (1)$$

96 Where: ICr = crystallinity index; I_{am} = diffraction intensity of amorphous portions;
97 I_{002} = diffraction intensity of peak of crystalline portion of plane 002.

98 **Wood samples**

99 Samples of *Enterolobium schomburgkii* (Fabaceae) wood with dimensions of 145 mm
100 x 80 mm x 20 mm were used in the tests. The samples were made available by a flooring
101 industry, the material was already presented in the form of a floor, with stable moisture content
102 (dry) and containing only heartwood. Despite being a durable wood, *Enterolobium schomburgkii*
103 was chosen, not only for the availability of samples, but also to value the species and encourage
104 nobler uses, such as floors and furniture, in addition to the traditional uses in Brazil in civil
105 construction.

106 Before the tests, the longitudinal surface of each specimen was polished with
107 sandpaper with grades 80 and 120 to avoid the influence of saw marks on the results. A total of
108 27 samples were evaluated. Samples were conditioned in a climate-controlled room in order to
109 reach the equilibrium moisture content ($12 \% \pm 1 \%$).

110

111

112 **Varnish**

113 Transparent water-based marine varnish (Sayerlack - YO.1371.00) was used, with satin
114 finish and $38,35 \% \pm 2 \%$ solid content. Based on the manufacturer's information, dilution must
115 be done with 10 % to 15 % water. So, tests were performed with three different dilutions: i)
116 varnish with only 10 % water; ii) varnish with further addition of 10 % bleached MFC; and iii)
117 varnish with addition of 10 % unbleached MFC.

118 Since the nanocellulose suspensions had low fiber concentration, and water is the largest
119 portion by volume, the same water density was applied in the calculation of MFC mass for
120 addition in varnish. Each solution was applied by brushing on nine 9 specimens per treatment,
121 totaling 27 samples.

122 After varnish solutions' application, samples were dried in a kiln with forced air
123 circulation for 4 hours and temperature of 25 °C, as recommended by the varnish manufacturer.
124 The samples were smoothed with 120-grit sandpaper and the varnish application and drying
125 was repeated twice. For each application, moisture weight applied to each specimen was
126 measured by weighing before and after brushing.

127 **Colorimetry**

128 Colorimetric characterization was performed with a Konica Minolta CM-5
129 spectrophotometer, operating in the range of 350 nm to 750 nm, with a xenon lamp, 8 mm
130 sensor aperture diameter, observation of 10°, and illuminant D65 (CIE Lab standard). Spectra
131 and colorimetric data were obtained for wood without treatments, at three different points per
132 sample for each varnish solution applied, for a total of 162 spectra/specimen.

133 In each sample, data were obtained from the longitudinal section, which provided the
134 values for L* (luminosity), a* (chromatic coordinates of the green-red axis), and b* (chromatic
135 coordinates of the blue-yellow axis). The values for C* (saturation) and h (hue angle) were
136 calculated according to Equations 2 and 3, respectively.

137
$$C^* = \sqrt{(a^{*2} + b^{*2})} \quad (2)$$

138
$$h = \arctan \frac{b^*}{a^*} \quad (3)$$

139 Total color variation ΔE^* was calculated based on Equation 4, to measure color
 140 changes after varnish application. This parameter can facilitate comparison because it
 141 represents three parameters in the CIE $L^*a^*b^*$ space (Ferreira and Spricigo 2017).
 142 Classification of ΔE^* is based on Table 1.

143
$$\Delta E^* = \sqrt{\Delta L^{*2} + \Delta a^{*2} + \Delta b^{*2}} \quad (4)$$

144 Where: ΔE^* = total color variation; ΔL^* , Δa^* and Δb^* = variation of luminosity and
 145 chromatic coordinates (treated sample – untreated sample).

146 **Table 1:** Wood total color variation (ΔE^*) based on Hikita *et al.* (2001) and Barreto and
 147 Pastore (2009).

ΔE^*	Classification
0,0 - 0,5	Negligible
0,5 - 1,5	Slightly noticeable
1,5 - 3,0	Remarkable
3,0 - 6,0	Appreciable
6,0 - 12,0	Very appreciable

148 **Wettability**

149 Wettability of samples was investigated by the sessile drop contact angle method with
 150 a drop shape analysis goniometer (Krüss). Three droplets (5 μ L) of distilled water were
 151 deposited on the longitudinal surfaces of each sample, through a syringe held perpendicularly
 152 to the surface. The contact angles were measured after 5, 15 and 30 seconds. All measurements
 153 were performed in the same experiment in an air-conditioned room at $20\text{ }^\circ\text{C} \pm 2\text{ }^\circ\text{C}$ and $60\% \pm$
 154 5% relative humidity, to avoid external influences.

155 The work of adhesion (WoA) is defined by the work required to separate the liquid
 156 from the solid surface, and can be measured by surface tension of the liquid (γ_{lv}) and contact
 157 angle (θ), according to the Young-Dupré equation (Schrader 1995) (Equation 5).

158 $WoA = \gamma_{lv}(1 + \cos\theta)$ (5)

159 ***Finishing tests***

160 a) Abrasion test

161 The abrasion was tested according to the Brazilian standard NBR 14535 (ABNT 2008),
162 in a Taber abrasion tester with CS17 grinding wheel. Two samples with dimensions of 100 mm
163 x 80 mm were used for each treatment. The wear rates were calculated based on difference in
164 weight before and after surface abrasion (Equation 6).

165 $WR = \frac{1000x(A-B)}{c}$ (6)

166 Where: WR = wear rate (mg/1000 cycles); A = Weight of samples before abrasion
167 (mg); B = Weight of samples after abrasion (mg); and C = number of cycles.

168 b) Coating adhesion

169 Coating adhesion was measured according to ASTM D4541 (ASTM 2017), with a
170 PosiTest AT-A pull-off adhesion tester. Three 20 mm diameter dollies were attached to each
171 sample with a two-component epoxy resin with minimum curing time of 24 hours before the
172 test. The coating/substrate adhesion tests were performed with the application of a constant rate
173 of 0,2 MPa/s to obtain the maximum coating resistance until the metal piece affixed to the
174 surface of the samples was peeled off.

175 c) Coating resistance to impact

176 The impact resistance of the coating was measured in accordance with NBR 14535
177 (ABNT 2008), adapted, which consists of assessing the damage caused by a steel ball with
178 diameter of 19 mm (± 1 mm) weighing 28 g (± 1 g) in free fall from 2 m above the specimen to
179 be tested. The assay was performed three times for each sample, totaling 27 tested areas. After
180 the collision of the steel ball, the specimens were analyzed in a 10x magnifying glass, and the

181 impact caused by the contact of the steel ball with the finished surface was quantified according
182 to Table 2.

183 **Table 2:** Graduation of the area affected by the impact of the steel ball, based on NBR 14535
184 (ABNT 2008).

Degree	Description
5	Light impact that leaves a smooth mark without cracks or fissures
4	One to two circular or semicircular cracks or fissures around the impact area
3	Moderate or severe cracks or fissures
2	Cracks or fissures extending out of the impact area, and/or slight film peeling
1	More than 25 % of film removed from the impact area

185 All tests were performed more than seven days apart after finish applications in a
186 climate-controlled room with a temperature of $20\text{ }^{\circ}\text{C} \pm 2\text{ }^{\circ}\text{C}$ and $60\text{ \%} \pm 5\text{ \%}$ relative humidity.

187 **Statistical analysis**

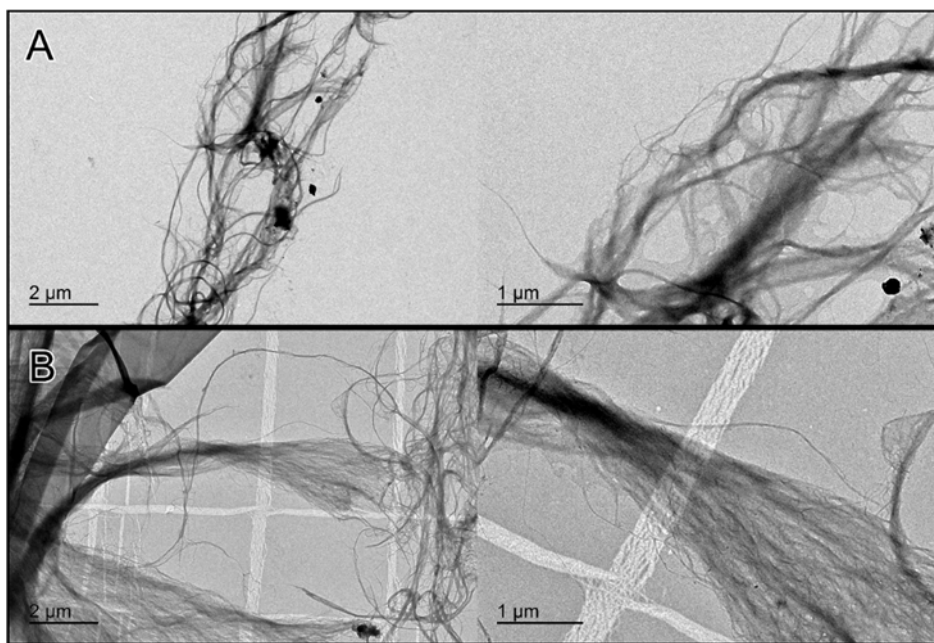
188 The data were submitted to analysis of variance and normality was determined. When
189 appropriate, the means were compared by the Tukey test at 5 % probability of error, to verify
190 if there were differences in the properties between the varnish with and without addition of
191 nanocellulose. The Sisvar 5.6 software (Ferreira 2008) was used in all the statistical tests.

192 **RESULTS AND DISCUSSION**

193 **Microfibrillated cellulose characterization**

194 Micrographs of cellulose nanofibrils obtained after 10 passes through the defibrillator
195 mill are shown in Figure 1. The average diameters of bleached and unbleached nanofibrils were
196 18,78 nm and 16,93 nm respectively, with no statistically significant difference. The average
197 thickness was close to the values found by Potulski *et al.* (2016).

198 The mechanical defibrillation process caused the cell wall fibers to fibrillate, reducing
199 their diameter and generating a structured network formed by nanofibrils. The diameter of
200 nanofibrils generally varies from 3 nm to 100 nm, depending on the origin of the cellulose, and
201 can have lengths greater than 1 μm (Dufresne 2013).



202
203 **Figure 1:** TEM images of cellulose nanofibers. (A) bleached, (B) unbleached.
204

205 The crystalline peak and amorphous halo intensities of bleached (BCF) and
206 unbleached (UCF) cellulose fibers and bleached (BMFC) and unbleached (UMFC)
207 microfibrillated cellulose are illustrated in Figure 2, and the average values found for the
208 crystallinity index (ICr) are reported in Table 3. The diffractogram contains a low intensity peak
209 in the 2θ region of 15° and a more intense peak in the 2θ region of 22° , which represent the
210 crystal planes for both cellulose fiber and MFC. These values agree with those reported by Silva
211 *et al.* (2019).

212 By determining the crystallinity index, it is possible to analyze the degradation
213 suffered by the fiber due to the mechanical defibrillation process. The crystallinity index of
214 cellulose refers to the number of crystalline regions, where the fiber has greater tensile and
215 elongation resistance, which directly influence the mechanical properties of the material
216 (Potulski *et al.* 2016).

217

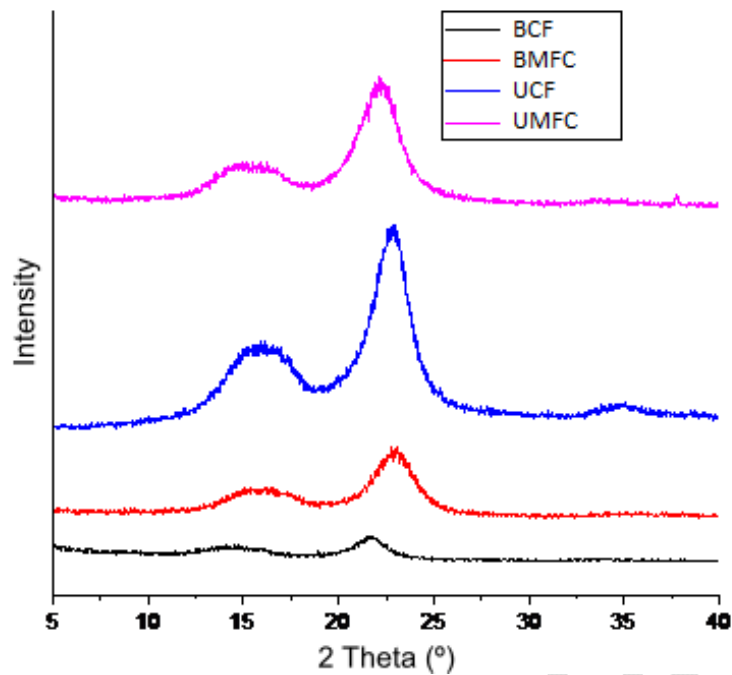


Figure 2: X-ray diffractogram of cellulose fibers and MFC samples.

Table 3: Crystallinity index of cellulose fibers and suspensions (MFC).

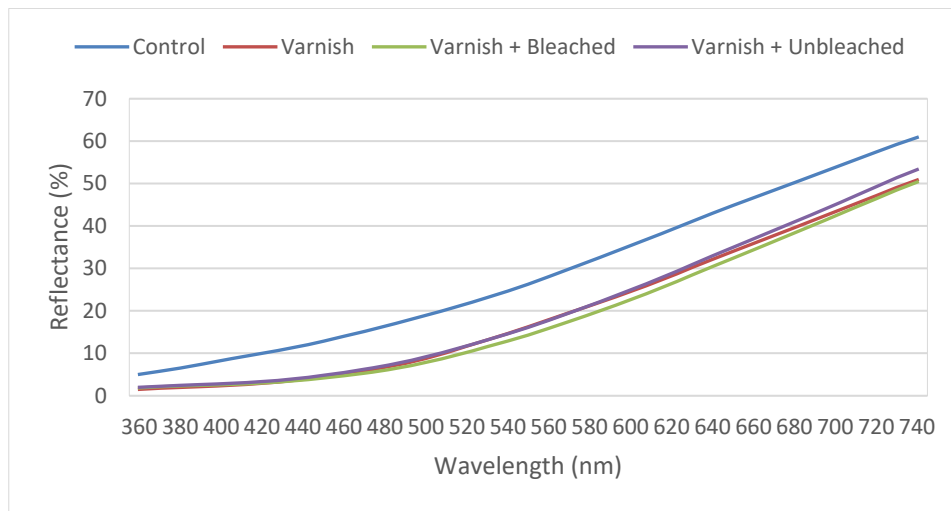
Sample	I_{002}	I_{am}	ICr
Bleached Cellulose	202	62	69 %
Bleached MFC	606	160	74 %
Unbleached Cellulose	1672	382	77 %
Unbleached MFC	1074	256	76 %

The bleached MFC had an increase in ICr after the mechanical defibrillation process, which resulted in greater exposure of the fibrils than in the cellulose fiber sample, increasing its ICr, but did not cause fiber degradation and tearing to the point of affecting the index. Lengowski *et al.* (2018) and Viana *et al.* (2019) found ICr values close to 80 % for unbleached pine cellulose fiber, near those found in work, which is consistent with other published studies.

One possible reason why the crystallinity index of the unbleached cellulose fiber and MFC is higher than that of the bleached cellulose is the delignification process. The bleaching process may have caused fiber degradation and consequently increased the reduction of the crystallinity index.

233 **Colorimetry**

234 Figure 3 shows the reflectance curve of the samples, revealing clear separation of the
 235 control wood curve from that of the finished samples. The colorimetric parameters of the
 236 samples without any type of coating (control) and with the coating are presented in Table 4.



237
 238 **Figure 3:** Visible reflectance spectra of evaluated samples.

239
 240 **Table 4:** Mean values and (standard deviation) of colorimetric parameters.

Treatment	L*	a*	b*	C*	h
Control	58,84 b (4,30)	10,24 a (1,43)	27,28 a (3,06)	29,19 a (2,99)	69,29 b (3,24)
Plain Varnish	47,58 a (6,21)	14,20 b (1,23)	37,30 b (5,53)	39,96 b (5,25)	68,81 b (3,23)
Varnish + Bleached MFC	45,72 a (4,30)	15,35 c (1,33)	35,58 b (4,02)	38,78 b (3,89)	66,51 a (2,41)
Varnish + Unbleached MFC	48,02 a (4,69)	14,71 bc (1,28)	36,08 b (4,59)	39,00 b (4,40)	67,61 ab (2,69)

Where: L* = luminosity; a* = green-red chromatic coordinate; b* = blue-yellow chromatic coordinate; C* = chroma; h = hue angle. Same letter in the column indicates no statistical differences at 5 % probability by the Tukey test.

241

242 The average brightness values (L*) showed that the application of the coating caused
 243 a reduction in the wood brightness, but there was no significant difference due to the addition
 244 of MFC to the varnish. This is advantageous because the addition of bleached or unbleached
 245 MFC did not change this property. The brightness reduction can be explained by the basic

246 characteristic of the chosen varnish. Since it is a satin (matte) varnish, it can cause a reduction
247 of the natural brightness of wood.

248 The coordinate a^* (red-green axis) is considered the main coordinate for wood color
249 change between species (Garcia *et al.* 2014). This coordinate presented statistically different
250 values for control wood, wood with varnish, and with varnish and bleached MFC, whereas the
251 finishing with varnish and unbleached MFC differed from wood without finishing. There were
252 no differences in the other treatments.

253 In general, the addition of the coating increased the value of a^* , intensifying the red
254 chromatic coordinate. Possibly some chemical present in the varnish absorbed a certain
255 wavelength in the visible range, so the color observed, as reflected, was complementary, as
256 described by Martins *et al.* (2015).

257 For parameter b^* , all finish treatments differed from the control sample, but did not
258 differ significantly from each other. There was also an increase in the b^* coordinate, indicating
259 intensification of the yellowish hue of the wood.

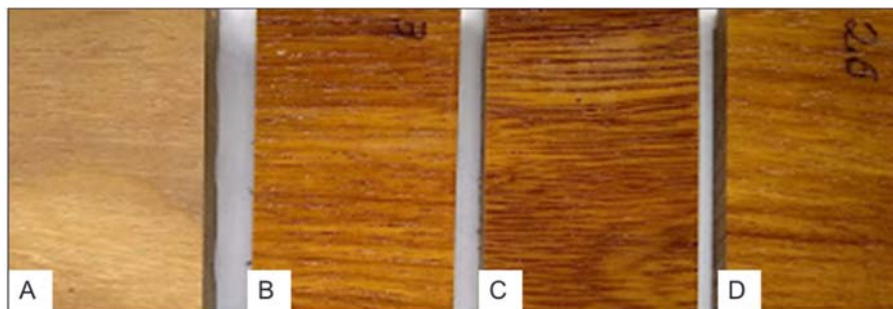
260 The total color variation (ΔE^*) determined by equation 4 considers the differences
261 between color coordinates and brightness (Table 5) and thus provides a broader view of color
262 variation between the coating types (Figure 4).

263 **Table 5:** Total color variation (ΔE^*) after finish application in contrast to plain varnish.

Treatment	ΔL^*	Δa^*	Δb^*	ΔE^*	Classification
Plain Varnish x Control	-11,26	3,96	10,01	15,58	Very appreciable
Plain Varnish x Bleached MFC	-1,86	1,15	-1,72	2,78	Remarkable
Plain Varnish x Unbleached MFC	0,45	0,50	-1,22	1,39	Slightly noticeable

264

265



266

267 **Figure 4:** Visual color variation: A) control wood; B) wood with plain varnish; C) wood with
268 varnish containing bleached MFC; D) wood with varnish containing unbleached MFC.

269

270 Figure 4 clearly reveals the wood color variation caused by the application of the
271 coating, reducing the brightness and increasing the color coordinates, intensifying the wood
272 hue. According to Table 5, the color variation of the samples containing plain varnish compared
273 to the control wood sample fits into the very appreciable classification, emphasizing the great
274 influence that the varnish has on ΔE^* , whereas the samples with bleached MFC compared to
275 the samples of plain varnish have a variation considered notable, but subtler than the variation
276 suffered by the sample when applying only the varnish. The same behavior occurred with
277 samples containing unbleached MFC, however, they were classified as slightly perceptible in
278 comparison with the plain varnish.

279 Although samples containing nanocellulose differed in the classification of the total
280 color variation, Vardanyan *et al.* (2014) stated that when exposed to weathering, wood coated
281 with varnish containing nanocellulose (1 wt% and 2 wt%) has better resistance to color
282 deviation caused by the absorption of UV light by the pulp, since the coating layer with
283 nanocellulose better protects the wood from weathering changes.

284 **Wettability**

285 The results of apparent contact angle (CA ($^\circ$)) are presented in Table 6 and Figure 5.
286 The contact angles from 5 to 30 seconds of the samples finished with plain varnish and with
287 varnish containing unbleached MFC increased more than the specimen treated with varnish
288 containing bleached MFC. This happened because the unbleached MFC contains lignin, which

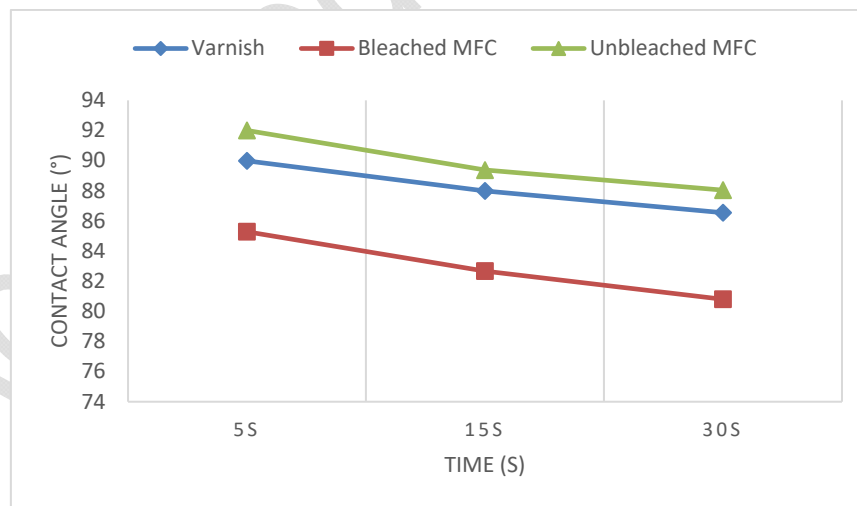
289 is a hydrophobic component. In the classification proposed by Ferreira (2013) at the time of 5
 290 seconds, the finish containing unbleached MFC was considered to be hydrophobic ($\Theta > 90^\circ$),
 291 but it was not significantly different than the plain varnish. Therefore, it can be said that at the
 292 time of 5 s, the unbleached MFC coating had hydrophobic character compared to the other
 293 treatments. For the other treatments and the other analyzed times, all coatings maintained
 294 hydrophilic character ($\Theta < 90^\circ$).

295 **Table 6:** Means values and (standard deviation) of apparent contact angle.

Treatment	Contact Angle ($^\circ$)			WoA (5 s)	Variation of CA (%)	
	5 s	15 s	30 s		5 s and 15 s	15 s and 30 s
Plain Varnish	89,98 a (4,98)	87,98 a (5,59)	86,54 a (5,67)	72,11 b (6,24)	-2,22 %	-1,64 %
Varnish + Bleached MFC	85,28 b (5,95)	82,66 b (6,10)	80,79 b (5,99)	78,00 a (7,39)	-3,07 %	-2,26 %
Varnish + Unbleached MFC	92,00 a (6,14)	89,37 a (7,21)	88,04 a (7,29)	69,59 b (7,68)	-2,86 %	-1,49 %

WoA = work of adhesion. Same letters in the row indicate no statistical difference at 5 % probability by the Tukey test.

296



297

298

Figure 5: Kinetics of the apparent contact angle for each treatment.

299

300

The work of adhesion (WoA) was measured after 5 seconds, which was the starting

301

point for all CA-linked analyses ($^\circ$). The WoA is the work necessary to separate the interface

302 from the equilibrium state of two phases. The decrease in the CA ($^{\circ}$) with time indicates
303 absorption or spread of water, so there will be an increase in the WoA coefficient, since the
304 water penetrated in the material will have a bond with the larger wood molecules and will
305 require greater work for separation.

306 When analyzing the contact angle variation between the 5 s and 15 s, the samples
307 finished with varnish without additives had the smallest contact angle reduction, while for the
308 times of 15 s and 30 s, the specimens coated with varnish containing unbleached MFC had
309 smaller variations.

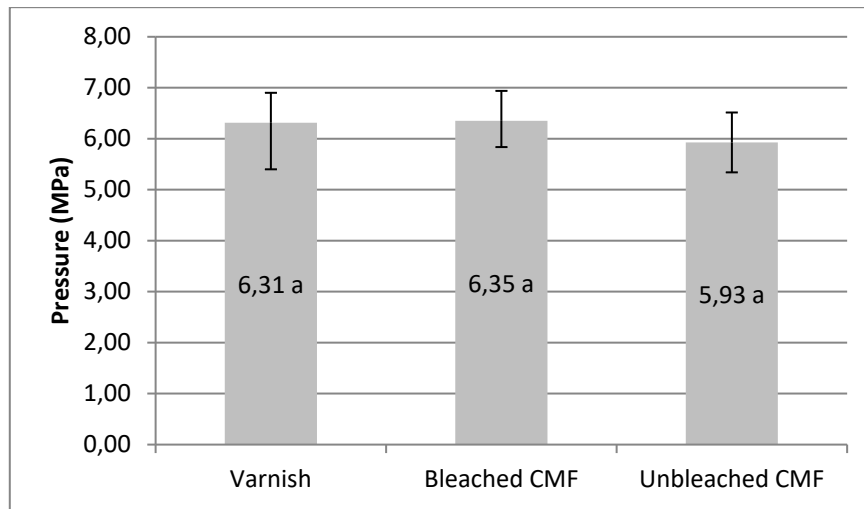
310 **Finishing test**

311 The wear rate (WR), referring to the abrasion resistance, was measured with 500 and
312 extrapolated to 1000 cycles per sample. The finish that had the highest wear rate, meaning the
313 largest mass loss after 1000 cycles, was the varnish without additive (0,031 mg/1000 cycles),
314 followed by treatment with varnish containing unbleached MFC (0,024 mg/1000 cycles), and
315 that with bleached MFC (0,017 mg/1000 cycles). However, none of the treatments showed
316 statistically significant differences at 5 %, i.e., the inclusion of MFC caused virtually no change
317 in the average wear rate, according to the standard, this test has no minimum requirement.

318 In the study by Veigel *et al.* (2014), the addition of microfibrillated cellulose and
319 cellulose nanocrystals in waterborne varnishes did not significantly improve the abrasion
320 resistance. This is because during the abrasion test, the coating layer is almost completely
321 removed, or can even be totally removed so as to expose the wood fibers over a comparatively
322 large surface area. Thus, this test measures the internal cohesion of the coating layer and to
323 some extent also the adhesion to the substrate.

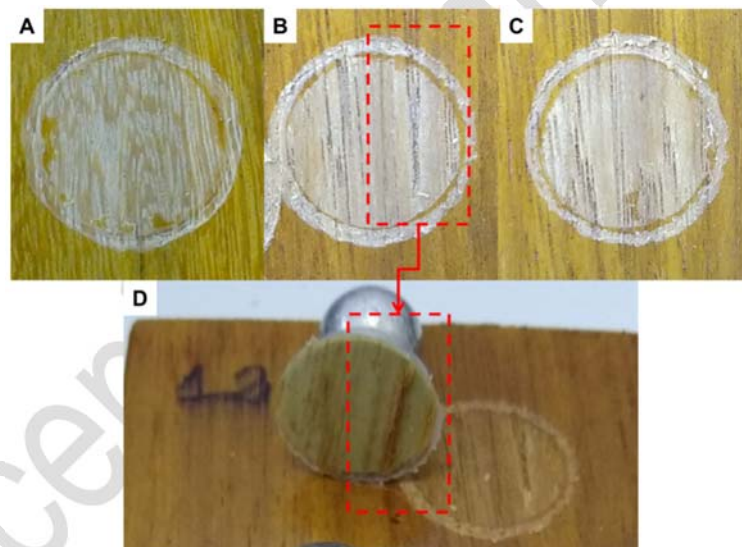
324 The results of the adhesion test indicated no significant numerical difference between
325 the plain varnish and the varnishes with the addition of the MFC solutions (Figure 6), but
326 visually the specimens coated with varnish containing MFC underwent greater particle pull-out

327 during the test (Figure 7). In other words, the finishes containing MFC had a greater penetration
328 and anchorage than the plain varnish, but this was not perceived numerically by the equipment.



329
330 **Figure 6:** Average values of adhesion test.

331



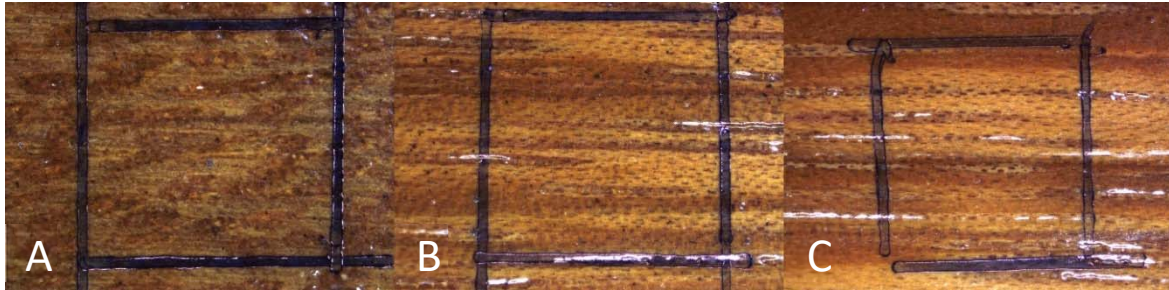
332
333 **Figure 7:** Particle pull-out in adhesion test: plain varnish (A), varnish with bleached MFC
334 (B), varnish with unbleached MFC (C), particles pulled out during the test, sample with
335 bleached MFC (D).

336

337

338 Poaty *et al.* (2014) performed the same test using cellulose nanocrystals (CNC) added
339 to the varnish, and obtained approximate results of 6 Mpa for the varnish with CNC, a result
similar to that found in this work.

340 In the impact resistance test, all samples had an impact degree of 5, respecting the
341 requirements of the standard for use in any category of furniture finishing, considered slight
342 impact, which can an almost imperceptible mark, without the presence of cracks (Figure 8).



343 **Figure 8:** Finishing with plain varnish (A), varnish with bleached MFC (B), varnish with
344 unbleached MFC (C). Images captured a 10x magnification.
345
346

347 The waterborne varnish had good ability to absorb the impact caused by the falling
348 sphere, preventing wood cracking. The same was observed by Fonte (2016), who classified the
349 impacts on wood coated with water-based varnish as grade 5.

350 The addition of MFC did not result in large variations in this test. The same degree of
351 impact was found for all three treatment types.

352 CONCLUSIONS

353 The optical coating characteristics, such as color, were not affected by the addition of
354 microfibrillated cellulose, and did not change the visual appearance when compared to samples
355 with plain varnish.

356 The changes in wood wettability were also small. There was no statistical difference
357 between the specimens coated with plain varnish and that containing unbleached MFC. But the
358 contact angle for the coating containing unbleached MFC increased, consequently producing
359 the best results.

360 In general, in the qualitative evaluation tests of the finish, the addition of nanocellulose
361 did not cause significant differences, but in the adhesion test, there was greater particle pull-
362 out, which could be the result of a better anchoring of the varnish to the wood.

363 It is possible to conclude the use of MFC as reinforcement in coatings has potential,
364 but tests with different consistencies and tests of other properties are necessary.

365

366

REFERENCES

367 **American Society for Testing and Materials. 2017.** ASTM D4541-17: Pull-Off Strength of
368 Coatings Using Portable Adhesion Testers. ASTM. West Conshohocken, PA, USA.
369 <https://www.astm.org/Standards/D4541.htm>

370

371 **Associação Brasileira de Normas Técnicas. 2008.** NRB 14535: Movéis de madeira -
372 Requisitos e ensaio para superfície pintadas. Rio de Janeiro, BR.
373 <https://www.abntcatalogo.com.br/norma.aspx?ID=762>

374

375 **Barreto, C.C.K.; Pastore, T.C.M. 2009.** Resistência ao intemperismo artificial de quatro
376 madeiras tropicais: o efeito dos extrativos. *Cienc Florest* 19(1): 23-30:
377 <http://dx.doi.org/10.5902/19805098416>

378

379 **Duan, H.; Shao, Z.; Zhao, M.; Zhou, Z. 2016.** Preparation and properties of environmental-
380 friendly coatings based on carboxymethyl cellulose nitrate ester & modified alkyd. *Carbohydr*
381 *Polym* 137: 92-99: <https://doi.org/10.1016/j.carbpol.2015.10.067>

382

383 **Dufresne, A. 2013.** Nanocellulose: a new ageless bionanomaterial. *Mater Today* 16(6): 220-
384 227: <https://doi.org/10.1016/j.mattod.2013.06.004>

385

386 **Ferreira, D.F. 2008.** SISVAR: um programa para análises e ensino de estatística. *Revista*
387 *Symposium* 6: 36-41: <http://www.dex.ufla.br/~danielff/meusarquivospdf/art63.pdf>

388

389 **Ferreira, L.M.V. 2013.** Revestimentos hidrofóbicos. Thesis (Master's degree), Universidade
390 Nova de Lisboa, Lisboa, Portugal. <http://hdl.handle.net/10362/11045>

391

392 **Ferreira, M.D.; Spricigo, P.C. 2017.** Colorimetria - Princípios e aplicações na agricultura. In
393 *Instrumentação pós-colheita em frutas e hortaliças*. Ferreira, M.D. (Technical Ed.). São Carlos:
394 Embrapa Instrumentação, Brazil. 209-220pp.
395 <https://www.bdpa.cnptia.embrapa.br/consulta/busca?b=ad&id=1084379&biblioteca=vazio&busca=autoria:%22SPRICIGO,%20P.%20C.%22&qFacets=autoria:%22SPRICIGO,%20P.%20C.%22&sort=&paginaAtual=1>

398

399 **Fonte, A.P.N. da. 2016.** Utilização da madeira de *Cryptomeria japonica* para a produção de
400 painéis colados lateralmente e aplicação de acabamento superficial. Thesis (Master's degree),
401 Universidade Federal do Paraná, Curitiba, PR, Brazil.
402 <https://acervodigital.ufpr.br/bitstream/handle/1884/46063/R%20-%20D%20-%20ANA%20PAULA%20NAMIKATA%20DA%20FONTE.pdf?sequence=1&isAllowed=y>

404

405 **Garcia, R.A.; Oliveira, N.S. de.; Nascimento, A.M. do.; Souza, N.D. de. 2014.** Colorimetria
406 de madeiras dos gêneros *Eucalyptus* e *Corymbia* e sua correlação com a densidade. *Cerne*
407 20(4): 509 – 517: <https://doi.org/10.1590/01047760201420041316>

408

- 409 **Gezici-Koç, Ö.; Erich, S.J.F.; Huinink, H.P.; Van Der Ven, L.G.J.; Adan, O.C.G. 2018.**
410 Understanding the influence of wood as a substrate on the permeability of coatings by NMR
411 imaging and wet-cup. *Prog Org Coat* 114: 135-144:
412 <http://dx.doi.org/10.1016/j.porgcoat.2017.10.013>
413
- 414 **Gibbons, M.J.; Nikafshar, S.; Saravi, T.; Ohno, K.; Chandra, S.; Nejad, M. 2020.** Analysis
415 of a wide range of commercial exterior wood coatings. *Coatings* 10: 1013.
416 <https://doi.org/10.3390/coatings10111013>
417
- 418 **Hikita, Y.; Toyoda, T.; Azuma, M. 2001.** Weathering testing of timber: discoloration. In *High*
419 *performance utilization of wood for outdoor uses*. Imamura, Y. (Ed.) Kyoto: Press-Net, Japan,
420 27-32pp.
421
- 422 **Islam, M.T.; Alam, M.M.; Zoccola, M. 2013.** Review on modification of nanocellulose for
423 application in composites. *Int J Innov Res Technol Sci Eng* 2(10): 5444–5451.
424 http://www.ijirset.com/upload/october/43_REVIEW.pdf
425
- 426 **Kluge, M.; Veigel, S.; Pinkl, S.; Henniges, U.; Zollfrank, C.; Rossler, A.; Gindl-Altmutter,**
427 **W. 2017.** Nanocellulosic fillers for waterborne wood coatings: reinforcement effect on free-
428 standing coating films. *Wood Sci Technol* 51(3): 601-613: [https://doi.org/10.1007/s00226-017-](https://doi.org/10.1007/s00226-017-0892-y)
429 [0892-y](https://doi.org/10.1007/s00226-017-0892-y)
430
- 431 **Lengowski, E.C.; Muñiz, G.I.B.; Andrade, A.S.; Simon, L.C.; Nisgoski, S. 2018.**
432 Morphological, physical and thermal characterization of microfibrillated cellulose. *Rev Árvore*
433 42(1): e420113: <http://dx.doi.org/10.1590/1806-90882018000100013>
434
- 435 **Martins, G.B.C.; Sucupira, R.R.; Suarez, P.A.Z. 2015.** Chemistry and Colors. *Rev Virtual*
436 *Quim* 7(4): 1508-1534: <http://dx.doi.org/10.5935/1984-6835.20150082>
437
- 438 **Poaty, B.; Vahe, V.; Wilczak, L.; Chauve, G.; Riedl, B. 2014.** Modification of cellulose
439 nanocrystals as reinforcement derivatives for wood coatings. *Prog Org Coat* 77(4): 813-820:
440 <http://dx.doi.org/10.1016/j.porgcoat.2014.01.009>
441
- 442 **Potulski, D.C.; Viana, L.C.; Muniz, G.I.B. de.; Andrade, A.S. de.; Klock, U. 2016.**
443 Caracterização de nanofilmes de celulose nanofibrilada obtida em diferentes consistências. *Sci*
444 *For* 44(110): 361-372: <http://dx.doi.org/10.18671/scifor.v44n110.09>
445
- 446 **Schrader, M.E. 1995.** Young-Dupre Revisited. *Langmuir* 11(9): 3585-3589:
447 <https://doi.org/10.1021/la00009a049>
448
- 449 **Segal, L.; Creely, J.J.; Martin, A.E.; Conrad C.M. 1959.** An empirical method for estimating
450 the degree of crystallinity of native cellulose using the X-ray diffractometer. *Text Res J*
451 29(10):786-94: <http://dx.doi.org/10.1177/004051755902901003>
452
- 453 **Silva, E.L.; Vieira, H.C.; Santos, J.X.; Nisgoski, S.; Saul, C.K.; Muñiz, G.I.B. 2019.**
454 Nanofibrillated cellulose, the small promising fiber: characteristics and potentialities. *Floresta*
455 49(3): 411 - 420: <http://dx.doi.org/10.5380/ufv.v49i3.58864>
456
- 457 **Tan, Y.; Liu, Y.; Chen, W.; Liu, Y.; Wang, Q.; Li, J.; Yu, H. 2016.** Homogeneous dispersion
458 of cellulose nanofibers in waterborne acrylic coatings with improved properties and unreduced

- 459 transparency. *ACS Sustain Chem Eng* 4(7): 3766-3772:
460 <https://doi.org/10.1021/acssuschemeng.6b00415>
461
- 462 **Vardanyan, V.; Galstian, T.; Riedl, B. 2014.** Effect of addition of cellulose nanocrystals to
463 wood coatings on color changes and surface roughness due to accelerated weathering. *J Coat*
464 *Technol Res* 12(2): 247-258: <https://doi.org/10.1007/s11998-014-9634-3>
465
- 466 **Veigel, S.; Gröll, G.; Pinkl, S.; Obersriebnig, M.; Müller, U.; Gindl-Altmutter, W. 2014.**
467 Improving the mechanical resistance of waterborne wood coatings by adding cellulose
468 nanofibres. *React Funct Polym* 85: 214-220:
469 <http://dx.doi.org/10.1016/j.reactfunctpolym.2014.07.020>
470
- 471 **Viana, L.C.; Muñoz, G.I.B.; Magalhães, W.L.E.; Andrade, A.S.; Nisgoski, S.; Potulski,**
472 **D.C. 2019.** Nanostructured Films Produced from the Bleached Pinus sp. Kraft Pulp. *FLORAM*
473 26(4): e20150191: <http://dx.doi.org/10.1590/2179-8087.019115>
474
- 475 **Yona, A.M.C.; Žigon, J.; Matjaž, P.; Petrič, M. 2021.** Potentials of silicate-based
476 formulations for wood protection and improvement of mechanical properties: A review. *Wood*
477 *Sci Technol* 55: 887–918: <https://doi.org/10.1007/s00226-021-01290-w>
478
- 479 **Žigon, J. 2021.** Interactions of a waterborne coating with plasma pre-treated densified beech
480 wood. *Eur J Wood Prod* 79: 1383–1394: <https://doi.org/10.1007/s00107-021-01716-z>